A Simple Model of the Atmospheric Response to ENSO Sea Surface Temperature Anomalies

R. KLEEMAN

Bureau of Meteorology Research Centre, Melbourne, Victoria, Australia

(Manuscript received 5 November 1989, in final form 17 June 1990)

ABSTRACT

A low-order tropical atmospheric model is developed that gives a reasonable account of the tropical precipitation and circulation anomalies observed during various El Niño and La Niña events. The dynamical part of the model is a linearization about a state of rest with the usual tropical vertical mode retained. The heating is obtained from latent and nonlatent sources with the former obtained from perturbing a steady-state moisture equation about climatology and confining the heating to high SST regions. A thorough sensitivity analysis is undertaken and the model tendency to place major anomalies on the western and northern side of SST anomalies is examined.

1. Introduction

In the last few years much attention has been focused on the depiction of the el Niño/Southern Oscillation phenomenon by coupled ocean–atmosphere models. This activity has ranged from simple conceptual models through to the very complex coupled AGCM/OGCM Experiments. In the midrange of complexity are the models of Anderson and McCreary (1985) and that of Cane and Zebiak (1987). The analysis of these models has provided some insight into which physical processes may be important to the coupled system [see Battisti (1988) for a further study of the latter model].

The atmospheric components of these models are highly simplified and it remains unclear to what extent these simplifications affect the results obtained. It is the intention here to develop a somewhat more realistic model in order both to understand better the ENSO atmospheric response and to provide an improved model for simple coupled experiments.

Central to developing a more realistic tropical atmosphere is the treatment of the moisture equation. A number of simple models with such an equation have been developed: Davey and Gill (1987) developed a time-dependent moisture equation forcing a time-dependent linear one-vertical mode atmosphere. Precipitation (and hence forcing) occurred in this model when specific humidity reached saturation at which point all of the moisture tendency was identified as precipitation. This model has been further refined by Budin and Davey (1989) who use a relative humidity criterion for deciding when precipitation occurs, and then use a simple parameterization based on the difference between the specific humidity and its saturation value to decide how much of the tendency goes into precipitation. Weare (1986) also used a moisture equation but assumed a steady state. This then enables precipitation to be defined in a straightforward manner. A complex iterative method was then used to obtain a steady state with the forced steady-state dynamical equations. Convergence to this state required that there be a negative feedback with respect to evaporation (it decreased as precipitation increased).

The above models attempt to reproduce the complete climatological state. The model of Zebiak (1986), used in the coupled model previously described, attempted only to produce perturbation quantities about some predefined climatological state (monthly mean winds). The model used an ad hoc moisture equation in which it was assumed that anomalous convergence developed in response to an evaporative anomaly (both provided forcing for the linear steady-state dynamical equations). This latter anomaly was related to sea surface temperature anomalies. The onset of the convergence was dependent on the convergence produced by the evaporative anomaly exceeding any background climatological divergence.

A different approach to that outlined above has been pursued by Neelin and Held in a series of recent publications (Neelin and Held 1987; Neelin 1988; Neelin 1990). It is argued that low-level convergence for a particular atmospheric column is given by the quotient of net moist static energy flux and the moist static stability of the column. In regions of high surface specific humidity the denominator is shown to be small while the opposite is the case for regions of low surface specific

Corresponding author address: Dr. Richard Kleeman, Max Planck Institut for Meteorology, Bundesstrasse 55, D-2000 Hamburg 13, West Germany.

humidity. The vertical velocity derived from this convergence is used to force a simple model of the boundary layer. Wind stresses are obtained by a consideration of the vertically integrated vorticity equation (which involves the boundary layer top vertical velocity) and a simple parameterization of surface wind stress in terms of boundary layer transports. A perturbation version about climatology has been used in coupled experiments.

The model to be developed here shall be, like the model of Zebiak (1986) and Neelin (1990), a perturbation about a background state (either climatological or the initial conditions for a coupled run). It has a steady-state full moisture equation which has been vertically integrated under the assumption that model variables are separable in this direction. In addition, the model shall use a moist static energy criterion for deciding when *penetrative* convection can take place. This convection will force a steady-state one-vertical-mode linear atmosphere. Due to the assumptions to be made concerning boundary layer relative humidity and temperature, the moist static energy criterion shall amount to an SST criterion. In addition to the latent heating, a nonlatent heating term proportional to SST anomalies will be utilized. This is intended to simulate the direct heating effects on the atmosphere of such anomalies. This term is important to the response obtained and is of the same form as that used by Davey and Gill (1987).

The model performance will be assessed using actual SST, wind, and outgoing longwave radiation (OLR) anomalies (the latter being a proxy for penetrative convection) from various ENSO and anti-ENSO episodes. Model sensitivity to the parameterizations adopted will be explored using the SST anomalies from the southern winter period of the 1987 ENSO event.

The paper is organized as follows: in section 2 the model equations will be derived and their physical justification given. In section 3 the model results will be compared with observations while section 4 contains the sensitivity study. A discussion of the parameterization of nonlatent heating may be found in section 5. Finally, conclusions and a summary may be found in section 6.

2. The model equations

The dynamical component of the atmosphere consists of the β-plane linear two-pressure-level model considered previously by Kleeman (1989) and its vertical structure is given in Fig. 1. In common with the steady-state model of Gill (1980), Rayleigh friction and Newtonian cooling are assumed in the momentum and thermodynamical equations, respectively. The Newtonian cooling is assumed to relax the 500 mb temperature perturbation towards the surface temperature perturbation. This latter modeling of the direct thermal effects of surface temperature changes is the same as that used previously in the literature by Gill (1985), Gill and Davey (1987), and Budin and Davey (1989). Its validity will be discussed further in section 5. The equations for the 750 mb quantities are

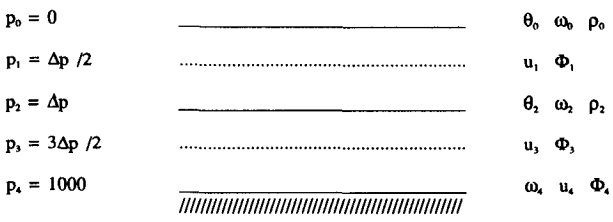

FIG. 1. The vertical deployment of physical variables in the model.

$$\epsilon u'_3 - f v'_3 = -\Phi'_{3x}$$

$$\epsilon v'_3 + f u'_3 = -\Phi'_{3y}$$

$$\epsilon(\Phi'_3 - R\,T'_4)/2 + c^2\nabla\cdot u'_3 = -R\,Q'_2/2 \quad (2.1)$$

where the superscripts refer to the particular level under consideration; Q is the heating rate (°K s^{-1}) at the middle level of the model (taken here to be 500 mb) while R is the universal gas constant. The shallow water speed $c = 59.3$ m s^{-1} for equal pressure intervals, and ϵ is the dissipation rate which has a value of 4×10^{-6} s^{-1} throughout this paper. The 250 mb quantities here have the opposite sign since the 500 mb heating does not force the mode with uniform vertical structure. These equations are completed by assuming an equatorial β-plane ($f = \beta y$). Note that the linearization is about a state of rest. Strictly, the linearization should take place about the basic state under consideration. This generalization will be omitted at present for the sake of clarity.

It was found that when the Eq. (2.1) were forced with observed heating anomalies (as deduced from outgoing longwave radiation (OLR) observations) the Pacific tropical wind anomalies produced were quite good when compared with observations. This was seen as sufficient justification for the value of ϵ used and the zero basic state linearization.

The midtropospheric heating rate Q'_2 in (2.1) is assumed to be given by a latent heating anomaly Q'_L and the major novel feature of the current work will be in the parameterization of this quantity: it has been known for some time observationally that in the equatorial region penetrative precipitation is located predominantly in areas where the SST is above approximately 27.5°–28°C (see, for example, Graham and Barnett 1987; Hirst 1986). This effect shall be incorporated into the present model by means of a surface–air critical moist static energy cutoff for such precipitation. Due to certain simplifying assumptions to be made later in text this cutoff shall amount to an SST cutoff, however the former criterion is preferred because it will allow more physically based generalizations of the current model.

Given the above discussion, it is clear that there are two possible mechanisms for inducing latent heating anomalies: first, they may be caused by changes in the moisture and circulation fields and second, there may be anomalies associated with certain regions attaining or dropping below the critical moist static energy. To reflect such changes, the following parameterization of the latent heating anomaly is adopted:

$$Q'_L = \begin{cases} \max(Q'_c, -\bar{Q}_p), & \text{if} \quad m(\bar{T}_4 + T'_4) > m_c \\ -\bar{Q}_p, & \text{otherwise} \end{cases} \tag{2.2}$$

where Q'_c is proportional to the change in precipitation due to changes in circulation and moisture fields, while $\bar{Q}_p$ is the basic state latent heating field. The quantity $m(T)$ is the moist static energy of a parcel of air at temperature T. The second line of (2.2) represents the shutting down of penetrative convection when the surface moist static energy drops below its critical value m_c. For the parameterization to be consistent it is required that the basic state latent heating vanish when $m(\bar{T}_4) < m_c$. Note that negative latent heating anomalies can never be less than minus the basic state latent heating.

The physical motivation for the moist static energy threshold is as follows: consider a surface air parcel lifted without entrainment and condensate loading (the assumed physical situation for penetrative convection) to the 700-mb level (the usual limit of trade cumuli). It can be shown (providing the density effects of water vapor are ignored) that the buoyancy/nonbuoyancy of the parcel depends on whether its moist static energy (MSE) is greater/less than the saturation MSE, m_{sat} of environment air at 700 mb. As θ_e^* generally decreases above 700 mb and does not regain its 700 mb value again until high in the troposphere,[1] it is clear that surface parcel able to buoyantly penetrate the 700 mb level will lift to almost the extent of the troposphere.

Parcels of air with surface MSE less than m_{sat} will, in general, be in regions with inversions below 700 mb (see Riehl 1979). Given that θ_e^* will usually have a negative gradient between inversion top and 700 mb, the surface parcel will have even more difficulty penetrating this region. It is assumed that penetrative convection is not possible in regions with such surface air. Conversely, in regions with surface air of MSE greater than m_{sat} it will be assumed that penetrative convection will be possible. This latter conclusion is not entirely obvious since such regions may possibly also have inversions below 700 mb. It will be assumed, however, that such surface air is sufficiently energetic either to eliminate such an inversion through cumulus activity or have sufficient vertical velocity (either from ascent below the inversion or from synoptic incursions) that it is able to penetrate any small remaining buoyantly unfavorable region.

Examination of temperature climatologies at 700 mb (Newell 1972; Oort 1983) reveals that in the oceanic tropical band 10°N–10°S the variations are considerably smaller than surface temperatures. Motivated by this the assumption is made that $m_c \equiv m_{\text{sat}}$ is constant. Given that as one moves to higher latitudes, the 700 mb temperature declines, one would expect that the model may unnecessarily shut down penetrative convection at these latitudes. This point will be further commented on in section 4.

The relationship between critical MSEs and critical SSTs comes about when the following assumptions concerning surface air are made:

$$T_4 = \text{SST} - 1.5°\text{C}$$
$$q_4 = 0.8 q_{\text{sat}}(T_4). \tag{2.3}$$

These assumptions are plausible over the tropical oceans, however, over land areas they are suspect and some kind of steady-state soil hydrology is probably required. For reasons of simplicity such parameterizations are omitted.

A 700 mb temperature of 10.3°C (not atypical of the equatorial region) means that the critical SST corresponding to the critical MSE is 28°C, which is in reasonable agreement with observations. Such a cutoff is adopted for the present model.

Returning to Eq. (2.2), note that the term $\bar{Q}_p$ can be constructed from observational data in a straightforward manner (more detail is presented later). To obtain Q'_c, three assumptions are made: first, the variables wind, moisture, and precipitation are assumed to have vertical structures which are independent of horizontal position (i.e., they are vertically separable). Second, it is assumed that the surface moisture and temperature fields are tied to SST via Eq. (2.3). Finally, the assumption is made that the moisture tendency term, like its dynamical counterparts, is zero. With these assumptions the moisture equation may be vertically integrated and solved for the 500 mb precipitation rate. If the basic state is taken to be $(\bar{u}_3, \bar{q}_4, \bar{T}_4)$ then the perturbation form of this equation may be written as

$$I_1 P'_2 = \rho_4 c_E \{ \overset{(1)}{W'_4 [q_{\text{diff}}(\bar{T}_4 + T'_4)]} \overset{(2)}{+ \bar{W}_4 [q_{\text{diff}}(\bar{T}_4 + T'_4) - q_{\text{diff}}(\bar{T}_4)]} \}$$
$$\overset{(3)}{+ I_2 [(\bar{q}_4 + q'_4) \nabla \cdot \mathbf{u}'_3} \overset{(4)}{+ q'_4 \nabla \cdot \bar{\mathbf{u}}_3}$$
$$\overset{(5)}{+ (\bar{\mathbf{u}}_3 + \mathbf{u}'_3) \cdot \nabla q'_4} \overset{(6)}{+ \mathbf{u}'_3 \cdot \nabla \bar{q}_4]}$$

[1] See, for example, Lee and Maher (1977) for typical tropical soundings upon which this statement is based.

with

$$q_{\text{diff}} \equiv q_{\text{sat}}(T_4) - q_4. \tag{2.4}$$

The labeling of terms here is for discussion purposes in section 4. Details of the vertical structure functions used and the values of I_1 and I_2 obtained therefrom may be found in the Appendix. Note that the bulk formula for evaporation [terms (1) and (2)] is used with the surface wind W_4 having a fixed minimum value of 4.8 m s^{-1}. This parameterizes short time scale variability. Obtaining Q_c' for use in Eq. (2.2) is now just a straightforward application of the diabatic heating formula:

$$Q_c' = L_v P_2'/c_p \rho_2. \tag{2.5}$$

The basic state latent heating $\bar{Q}_p$ is obtained as follows: Arkins' formula (K. Puri, private communication) relating precipitation to OLR,

$$P = \max[0., 0.175\ (280\text{-OLR})]\ \text{mm day}^{-1} \tag{2.6}$$

(OLR is measured in W m^{-2}), is used to construct a monthly mean tropical (30°N–30°S) rainfall climatology from a 1974–1986 OLR dataset (NOAA-9 satellite data). The estimate of tropical rainfall by Eq. (2.6) is naturally subject to uncertainties given the crudeness of the algorithm used to calculate it. Some indication of the accuracy and limitations of such methods may be found in Arkin and Meisner (1987). It is also not clear from such data which proportion of the precipitation is penetrative and which is due to trade cumuli. Evidently, to obtain such detail requires more sophisticated techniques. In the absence of long datasets incorporating such distinctions the following approach has been adopted:

$$\bar{P}_p = \begin{cases} 0.8\bar{P}, & \text{if } m(\bar{T}_4) > m_c \\ 0, & \text{otherwise.} \end{cases} \tag{2.7}$$

The quantity $\bar{Q}_p$ is now obtained using the assumed vertical structure function for P and the diabatic heating formula.

The solution of the model is calculated using an iterative technique similar in concept to that used by Webster (1981). Specifically, the following method is used: the mean quantities $\bar{T}_4$ and $\bar{\mathbf{u}}_3$ are calculated using the Reynolds SST climatology and the 1980–86 ECMWF 850-mb wind climatology (monthly mean values are used). Equation (2.3) is then used to calculate $\bar{q}_4$. It was found necessary to calculate the mean divergence field separately because the field obtained from the ECMWF analysis was too noisy. It is calculated from the tropical precipitation climatology previously constructed and the basic state version of (2.4) with appropriate mean quantities inserted.

The SST anomalies used to force the model are the NMC/CAC anomalies. These are used in conjunction with (2.3) to calculate T_4' and q_4'. All of the terms on the right-hand side of Eq. (2.4) are then calculated with $\mathbf{u}_3'$, the anomalous circulation, set to zero. The shallow-water set of equations is then solved with the corresponding forcing. The $\mathbf{u}_3'$ obtained is then used to recalculate the right-hand side terms and hence a new forcing for the shallow-water set is obtained. This process is iterated until a steady state is obtained. After each iteration a simple 5-point filter of the form

$$P'_{mn} = P_{mn} + [P_{mn+1} + P_{m+1n} + P_{m-1n} + P_{mn-1} - 4P_{mn}]/8 \tag{2.8}$$

is applied to the precipitation field. This is intended to crudely parameterize mesoscale convective system movement. The filter has the effect of smoothing the ultimate precipitation field and has only a minor effect on the large-scale wind field obtained.

3. Model results

In the first set of results to be described, the model was forced with three monthly meaned SST anomalies from the 1982/83 ENSO event, the 1987 event, and finally the 1975 anti-ENSO event. The value of "SST" anomalies over land areas was taken to be zero while the mean SST over land was set at the interpolated value used in the Reynolds NMC/CAC SST climatology.

The model results from February, March, and April 1983 can be seen in Fig. 2. For comparison, the FSU surface wind anomalies and the OLR anomalies [converted to precipitation using (2.6)] for the same period are also displayed. As can be seen, the model does a good job in delineating the major areas of enhanced and suppressed convection. Some deficiencies of detail are apparent: the suppression of convection in the western Pacific is somewhat too weak in the model, and the positions of the peak positive precipitation anomalies in both the Pacific and Indian oceans are displayed somewhat from where observations place them. The modeled wind field is in quite reasonable agreement with observations albeit somewhat too weak. Strong equatorial westerly anomalies with a southerly component extend from the dateline to around 125°W, easterly anomalies are apparent in the Indonesian region, and in the mid-South Pacific (20°S, 140°W) in both model and observations. One difference in the wind fields occurs in the far eastern Pacific where observations suggest that no anomalies are present while the model has easterlies to about 90°W (on the equator). A similar deficiency was noted in the model of Zebiak (1986), although the "spurious" easterly anomalies here are much less pronounced. With regard to the SST cutoff of convection employed in the model, it is interesting to note that in the general area marked by a cross in Fig. 2, SST anomalies are quite large (1°–2°C) and yet in both model and observations there is no anomalous penetrative convection. The avoidance of this area by both model and observational precipi-

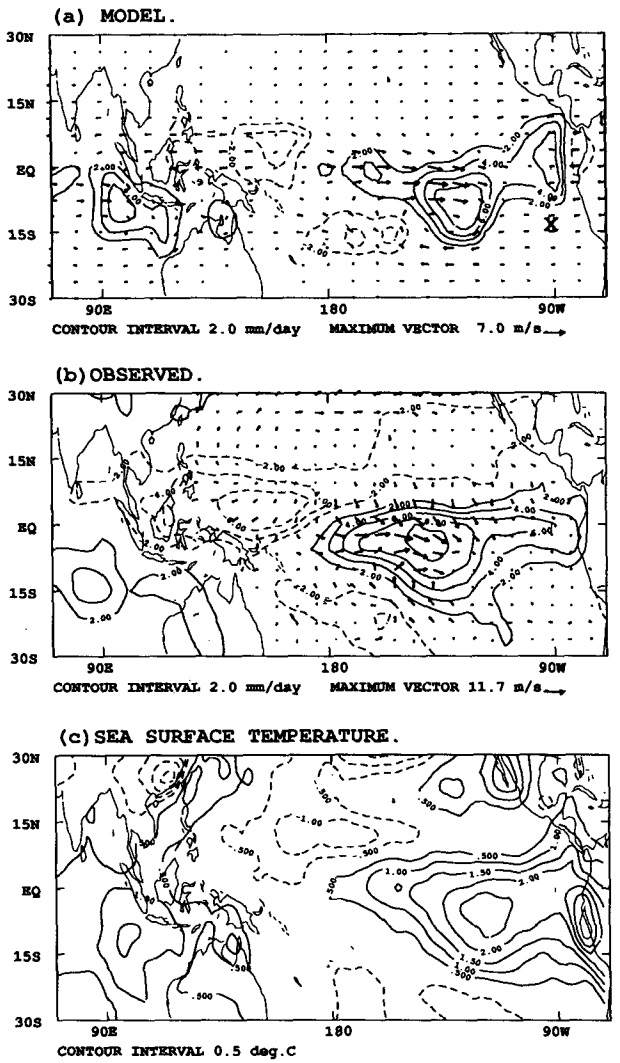

FIG. 2. The modeled and observed precipitation and wind fields for February–April 1983 together with the NMC/CAC SST anomaly analysis for the period. The contour interval for the precipitation fields is 2 mm day^{-1} while for the temperature field it is 0.5°C. (a) The modeled precipitation and wind anomalies (adjusted to the 1000-mb level), (b) the observed anomalies (FSU surface winds), and (c) SST anomalies.

tation is very similar in geographical form. This point will be discussed further in the next section.

In Fig. 3 the analogous results from June, July, and August 1987 are shown. As can be seen, the model response for the Pacific in precipitation is in reasonable agreeement with observations; a strong positive anomaly in precipitation is evident just west of the dateline in both model and observations, this anomaly extends eastward in the vicinity of the ITCZ in both fields, the negative precipitation anomalies to the south and north of the equator are reasonably represented in the model, although the northern anomaly extends further south in the model than observations, and associated with this the westward extension of the dateline positive precipitation anomaly is absent in the model. In the Indian Ocean region, the model appears to be reacting

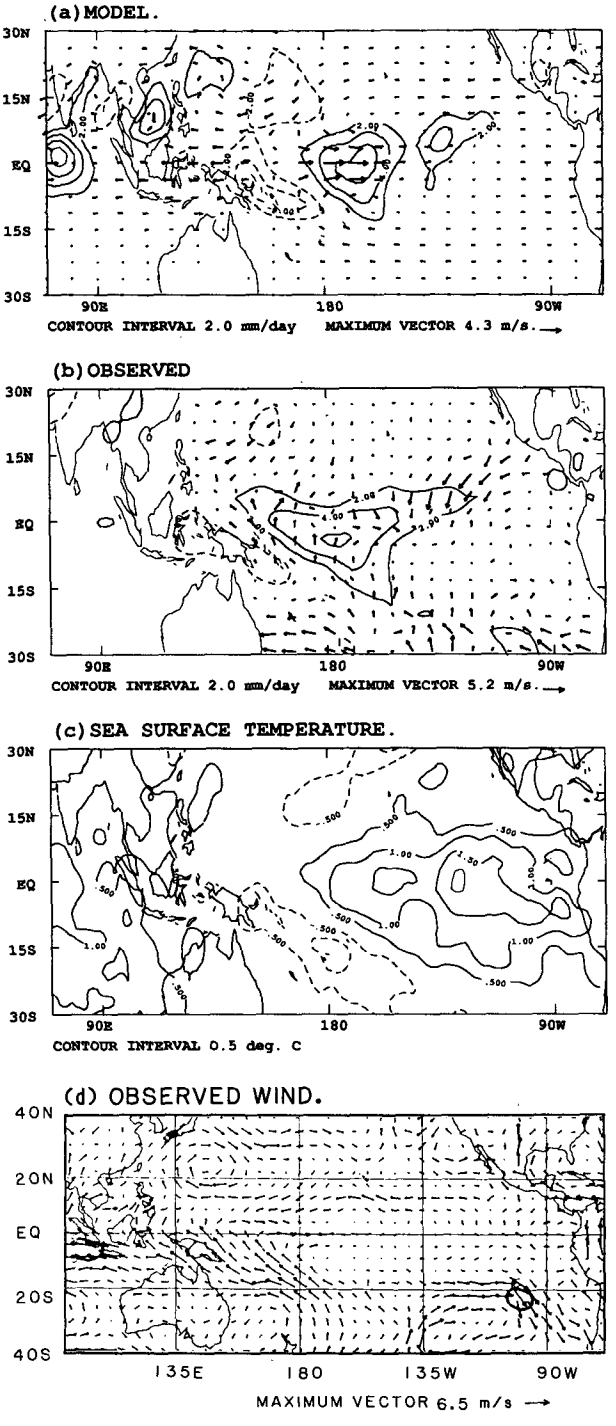

FIG. 3. Similar to Fig. 2 except for the months June–August 1987. The precipitation contour here is reduced to 2 mm day^{-1}. (a) The modeled anomalies, (b) the observed precipitation anomaly, (c) the SST anomaly, and (d) the NMC 850-mb anomalies.

too strongly south of India. The NMC analyzed 850-mb wind anomalies are also included in Fig. 3d, as there are significant qualitative differences between these and the FSU surface analysis displayed in Fig. 3b; thus, for example, the strong equatorial westerly wind anomalies seen around the dateline in the NMC analysis are very weak in the FSU analysis. Also, the strong northerly anomalies seen in the FSU analysis in the vicinity of 5°N, 140°W have no counterpart in the NMC analysis. Whether such differences are due to genuine differences in the 850-mb and surface conditions at the time is unclear, certainly if they are, they are beyond the scope of the current model. Much better agreement is obtained when the model results are compared to the NMC analysis. Note that the model winds in 3a are for the surface. At 850 mb the winds are simply scaled up so the maximum wind vector is 6 m s^{-1}. The model and observations show general agreement in the Pacific with near dateline westerlies, SPCZ easterlies, an anticyclonic anomaly centered at around 20°N, 160°E, and easterly anomalies in the Indonesian region and also further east in the ITCZ of the eastern Pacific. Some deficiencies of detail are apparent with the SPCZ anomalies being underestimated in the model. This particular point will be discussed further in section 4. Again, it is worth pointing out that both model and observations avoid placing significant positive precipitation anomalies over some very substantial positive SST anomalies in the eastern Pacific. This point is analyzed in detail in the next section.

Figure 4 shows the same quantities for the southern spring of 1975. Considering, first, the precipitation field, it is seen that the longitudinal placement of anomalies is quite good with negative anomalies being centered around 170°E in both model and observations, positive anomalies in the Indonesian region in both, and negative anomalies in the Indian Ocean equatorial region, although the model response here was overdone compared to observations. The deficiencies in agreement, apart from this, were the northward extension of anomalies in the model in the western Pacific, particularly the positive anomalies east of the Philippines. It is interesting to note that again there are substantial SST anomalies in the central and eastern Pacific which are causing very little precipitation response in model and observations. Turning to the wind anomalies one sees that there is substantial agreement in the positioning and strength of the major equatorial Pacific anomalies; easterly anomalies (strengthened trades) are apparent from the dateline to the Indonesian region in both model and observations. The modeled westerly anomalies in the far eastern Pacific are not as strongly apparent in the observations, although there is some indication of them. No doubt the presence of the Andes here complicates matters.

The second set of experiments involved forcing the model with SST anomalies (a 3-month running mean was used) from three, 12-month periods: January–December 1975; June 1982–May 1983; and January–December 1987. Thus, a strong and a moderate warm event, together with a moderate cold event, were analyzed. The data collected were the 5°N–5°S averages of precipitation and zonal wind. The Hovmoller diagrams of modeled and observed quantities may be seen in Figs. 5–7. The verifying winds are the FSU product.

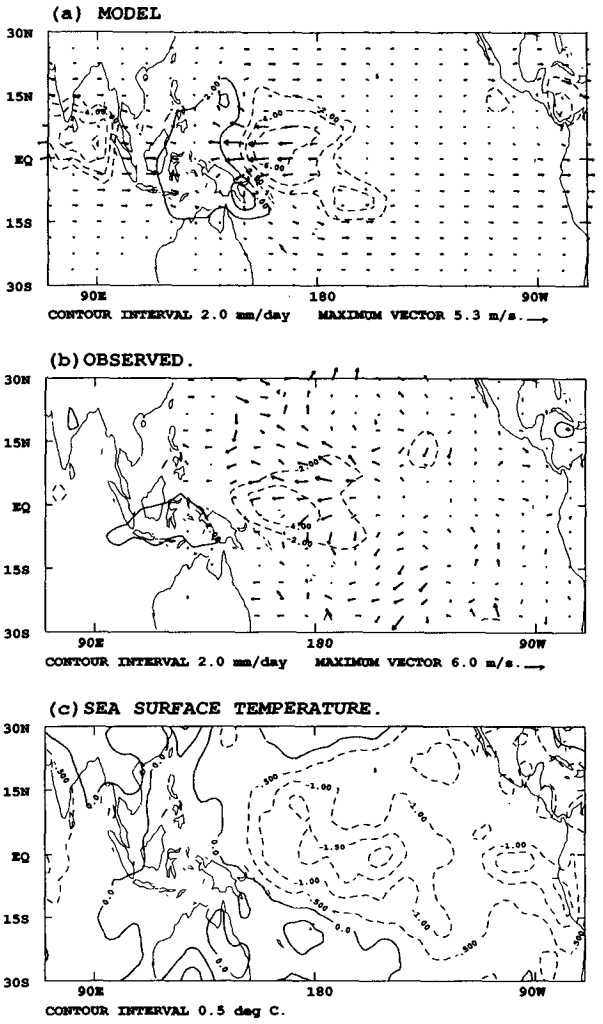

FIG. 4. Similar to Fig. 2 except for the months September–November 1975. The precipitation contour here is 2 mm day^{-1}. (a) The modeled anomalies, (b) the observed precipitation and wind anomalies, and (c) the SST anomaly field.

Focusing first on the 1975 cold event, reasonable general agreement is seen between observations and model results in both fields; thus, there is suppressed convection near the dateline for most of the year in both model and observations, enhanced convection in the region of 130°E in both, and suppressed convection in the Indian Ocean around 85°E. The model appears to be estimating the dateline and 130°E anomalies reasonably well but overestimating the Indian Ocean suppression. Both model and observations agree on

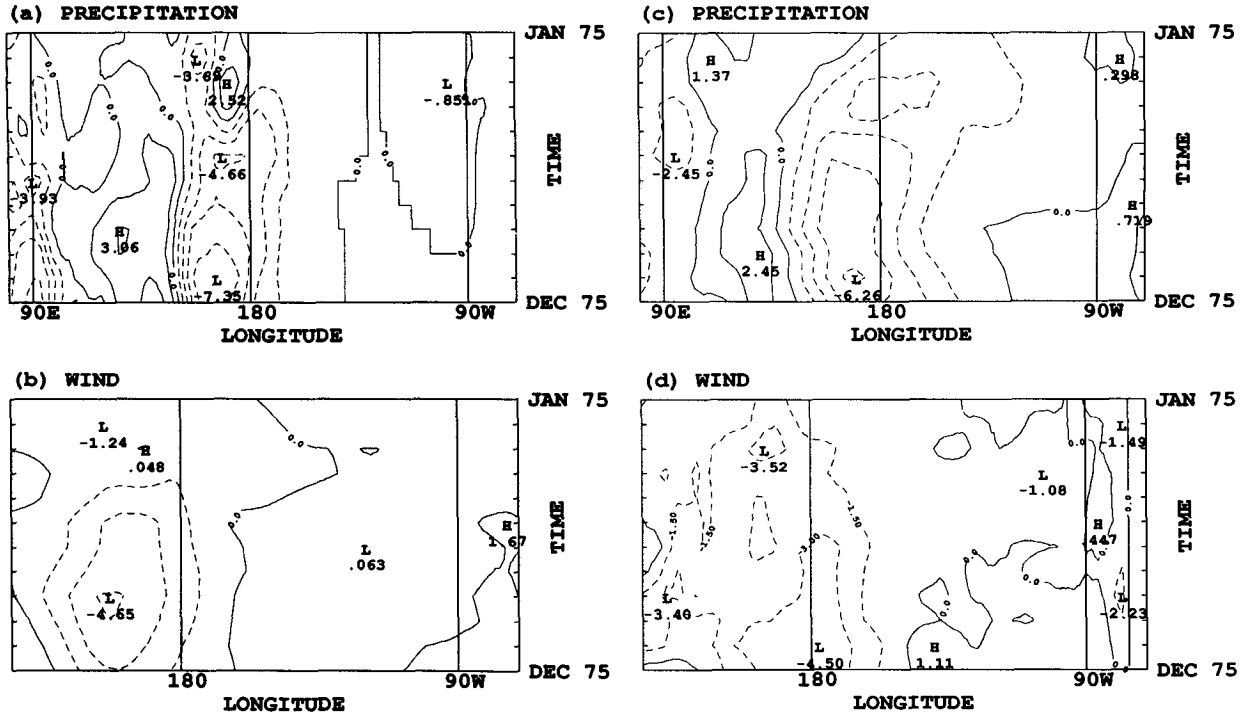

FIG. 5. A time–longitude section of precipitation and wind anomalies for 1975. The section is obtained by averaging values between 5°N and 5°S. (a) The modeled precipitation anomaly, (b) the model wind anomaly (surface value), (c) the observed precipitation anomaly, and (d) the observed FSU surface wind anomaly. The contour intervals are 1.5 mm day^{-1} for precipitation and 1.5 m s^{-1} for wind.

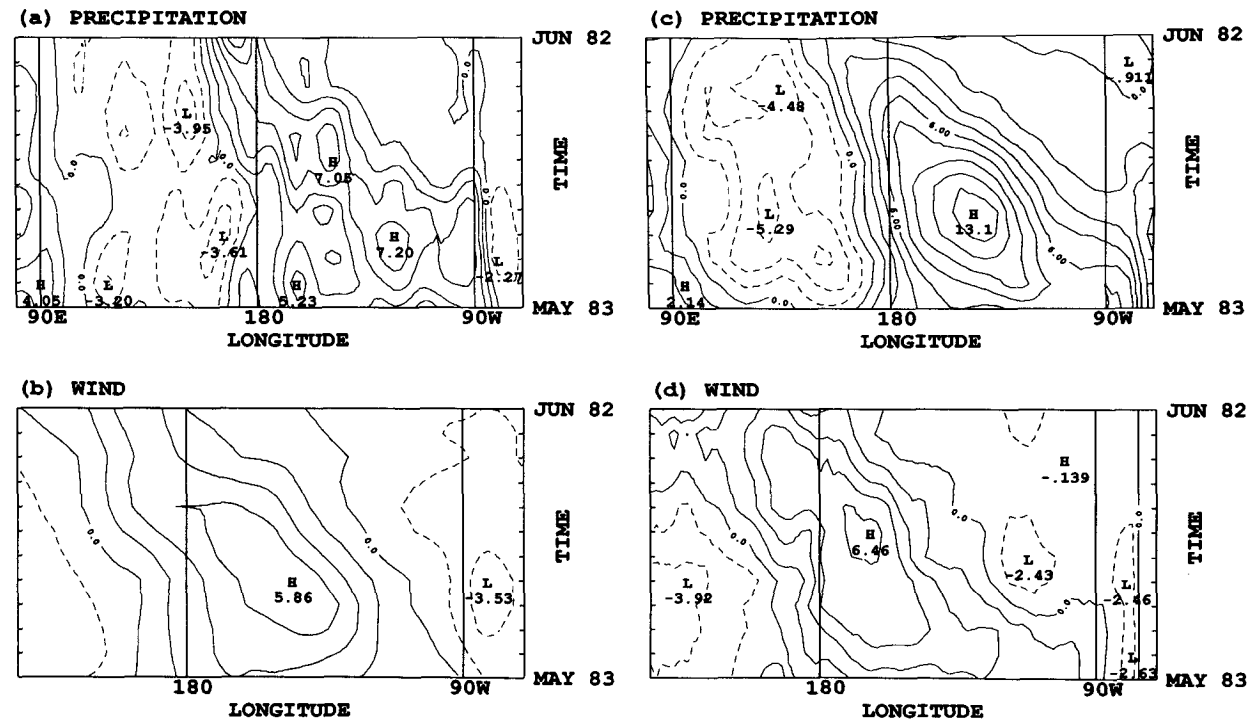

FIG. 6. Same as Fig. 5 but for the period June 1982–May 1983.

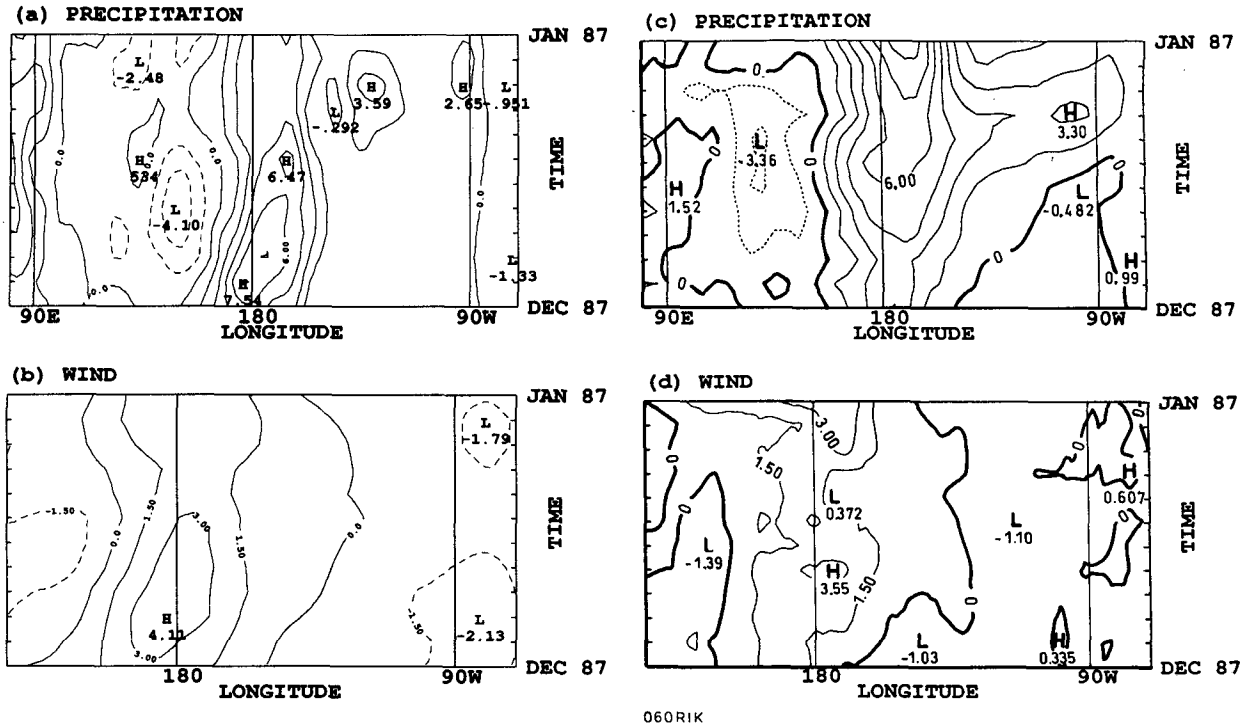

FIG. 7. Same as Fig. 5 but for 1987.

the general strengthening of anomalies towards the end of the year. With respect to the wind anomalies, in both observations and model there are easterly anomalies in the western Pacific region. Towards the end of the year, the observed anomalies are greatest near the dateline, whereas the model tends to place the largest anomalies further to the west around 160°E. Note, also, that both model and observations tend to have weak westerly anomalies in the eastern Pacific with this effect becoming more pronounced towards the end of the year.

Similar Hovmöller diagrams for 1982/83 can be seen in Fig. 6. For this period there appears to be good agreement between the modeled and observed winds, although the modeled westerly anomalies appear to be slightly weaker than observations. Both the model and observations place the strongest westerly anomalies in the southern summer and the easterly progression of the anomalies appears to be quite well modeled. There is somewhat of a discrepancy at the end of the time period where observations suggest more of a weakening of the westerly anomalies than does the model.

The precipitation anomalies do not appear to show quite the same degree of agreement with the modeled anomalies being generally weaker than observations. The modeled response also appears to be somewhat noisier. Qualitatively, however, the model and observation anomalies show reasonable agreement; easterly progression of both positive and negative anomalies are well estimated and the spreading of large positive anomalies across to 90°W occurs around the same time. The position and strength of Indian Ocean anomalies seem in reasonable agreement, also.

The final period considered was the moderate ENSO of 1987. The Hovmoller diagrams appropriate to this period may be seen in Fig. 7. In comparing modeled and observed precipitation it is seen that there is reasonable agreement with regard to the longitudinal placement of anomalies; there is virtually no eastward progression of anomalies as observed and modeled for the 1982/83 ENSO. In both model and observations there is some indication of an eastern Pacific response during the early months. The main discrepancy between model and observations is in the temporal evolution of the event with near dateline positive anomalies being strongest at the beginning of 1987 in the observations and at the end of that year in model results. In this regard it is interesting to note that the unsmoothed monthly OLR anomalies reveal that at the beginning of the year there were quite intense oscillations between positive and negative values from month to month in the Indonesian to dateline region. This transient activity (presumably evidence of the 30–60-day oscillation) in the real atmosphere may have been significant in influencing the longer time scale response and causing it to differ from the present steady-state model. The above comments concerning the precipitation field are broadly the same for the wind field. The longitudinal placement of anomalies in the model is in general agreement with observations with perhaps the model

easterlies in the eastern Pacific being displaced too far east. The temporal evolution of the westerly anomalies showed the same pattern of discrepancy previously noted with regard to the precipitation field; peaking early in the observations and late in the model (there is, however, some indication of a late peak in the observations, also). On the other hand, the easterly anomalies in the western Pacific seemed in reasonable temporal agreement with the modeled wind being perhaps too strong. The modeled easterlies in the east were also a little strong.

4. Model sensitivity experiments

In the first set of experiments to be described, the terms contributing to the anomalous precipitation in areas with above the critical SST [see Eq. (2.4)] were examined for their effect on the final penetrative precipitation anomaly. Their effect was assessed by forcing the model with the southern winter 1987 SST anomaly and successively switching off the various terms (there are six of them in all). The differences this made to the ultimate precipitation field obtained can be seen in Fig. 8 (a negative value implies that switching off the term resulted in decreased precipitation and vice versa). Only the Pacific basin was considered in the sensitivity experiments to follow.

The most significant response obtained was when term (3) was switched off when a large amount of the precipitation response disappeared. This term is analogous to the convergence feedback term used by Zebiak (1986). It differs from that used by this author in that the anomalous divergence in Zebiak's model was multiplied by a *constant* parameter β, whereas, here, the

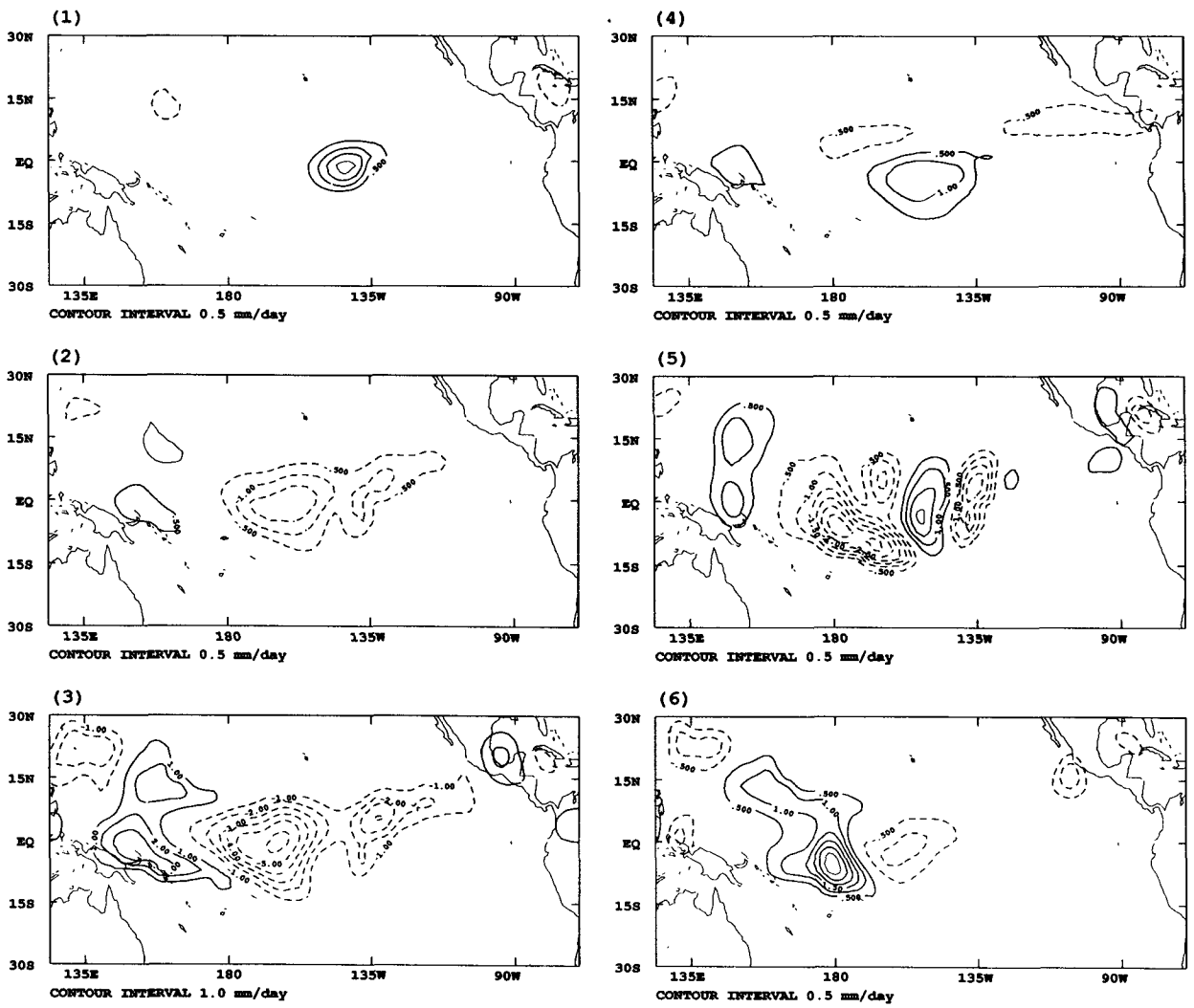

FIG. 8. The difference fields in precipitation resulting from artificially suppressing the terms in the moisture perturbation equation (see the text). The contour interval in all cases except (3) is 0.5 mm day^{-1}. In the exceptional case it is 1.0 mm day^{-1}. The labeling of diagrams indicates the particular term suppressed in Eq. (2.5).

multiplying factor involves $\bar{q}_4 + q'_4$, which because of the dependence of q_4 on the SST, varies horizontally. Thus, one would expect the "moisture convergence feedback" in the present model to operate more efficiently in regions with higher SST. This particular point is examined further.

Of the other terms considered, term (5) was perhaps the strongest. It acted to strengthen the western side of the dateline precipitation anomaly and weaken somewhat the eastern side. This effect was canceled to some extent by the other moisture advection term (6), although the net effect of these terms (not shown) was to strengthen the anomaly by about 1.0–1.5 mm day^{-1}. It is worth noting that when a similar study to the present one was conducted with the February–April 1983 anomaly, term (5) was similarly important to the main positive anomaly obtained and there was then less cancellation by term (6).

The effect of the evaporation terms (1) and (2) is of some interest given the emphasis placed in the literature on the connection between evaporation and SST anomalies.

It is clear that only term (2) is important to the positive anomaly, but it is responsible for at most 2.0 mm day^{-1} of the total response. Note that the evaporation anomaly *by itself* is probably responsible for only a fraction of the 2.0 mm day^{-1} since this figure represents the effects of the moisture convergence feedback as well. The above weak response was also noted in the 1983 experiments previously mentioned.

Examination of term (2) in Eq. (2.4) reveals that it is the change in q_{diff}, the difference between surface air specific humidity and saturated SST specific humidity, that causes the evaporation effect previously described. It may be that the current model underestimates this change by making the assumptions contained in Eq. (2.3). To examine this possibility, anomalies in q_{diff} were constructed using the COADS data for specific humidity (together with the SST climatology and anomaly analysis used previously); a climatology of q_{diff} for the period 1950–1979 was constructed and then anomalies were computed for the February–April period of 1983. A comparison with the values of anomalous q_{diff} predicted by Eq. (2.3) revealed that the observations were approximately 50% larger in some of the regions of high SST and precipitation anomaly. However, even with Δq_{diff} values artificially inflated in the model by 50%, the evaporation was unable to account for any more than about 40% of the total response obtained.

The other evaporation term (1) acts to suppress convection in the equatorial area around 140°W. This effect is presumably due to the reduction in the trades caused by westerly anomalies in the area; the trades are sufficiently strong here that a reduction will register as a reduction in evaporation which has a minimum built in wind speed of 4.8 m s^{-1}.

It is worth pointing out that evaporation changes affect the model response indirectly in that when the SST changes, the specific humidity field changes also because of Eqs. (2.3). Evaporation is clearly the physical mechanism by which this change in the humidity field takes place. It is the change in the *steady-state rate* of evaporation, however, that is being estimated by terms (1) and (2) in Eq. (2.4). This particular point will need to be kept in mind when the current model is used in coupling experiments.

The final term considered (4), was of smaller importance to the response than the other terms considered.

In the second set of sensitivity experiments conducted, the other factors affecting the final response were examined. First, the nonlatent heating term $Q'_{\text{NL}} \equiv \epsilon R T'_4/2$. in Eq. (2.1) was switched off and the differences this made to the precipitation and wind fields computed. The results can be seen in Fig. 9a. It is apparent that there is a substantial shutdown of the response; the main positive precipitation anomaly just west of the dateline has been reduced by perhaps 70%. There is also some removal of the negative precipitation anomaly in the western Pacific, although the effect here is substantially less pronounced. The wind field difference looks qualitatively similar (with sign reversed) to the original field (displayed for reference in Fig. 9b) but with magnitude in the central Pacific reduced by around 30%. Thus, about 70% of the wind field appears to result from the presence of Q'_{NL}. Of course one should not conclude that Q'_{NL} *directly* causes such a response in the wind field since moist convergence feedback processes are clearly important in the current model. To illustrate this point clearly, the wind field directly resulting from Q'_{NL} is shown in Fig. 9c [i.e., Eq. (2.1) forced only by Q'_{NL}]. As can be seen, the direct wind response is substantially less with westerly anomalies produced being around 20% of the full response.

In the next experiment, the effect of the penetrative convection shutdown mechanism was examined. This is the negative precipitation anomaly that results from the SST dropping below the critical value for penetrative convection [the second line of Eq. (2.2)]. To examine this, the negative precipitation value inserted in the model when the SST was reduced below this critical value was artificially set to zero and the difference which this made to the precipitation and wind fields computed. The results can be seen in Fig. 9d where it is immediately apparent that the greatest effect is in the western Pacific where a large amount of the negative precipitation anomaly is removed. The effect on the wind field is to substantially reduce the easterly wind anomalies in the Indonesian region and to reduce the anticyclonic circulation at 20°N, 160°E. The effect on the equatorial westerly anomalies in the central Pacific is far less pronounced with some slight diminution being apparent. A possible explanation for this latter result is that the negative precipitation anomalies in

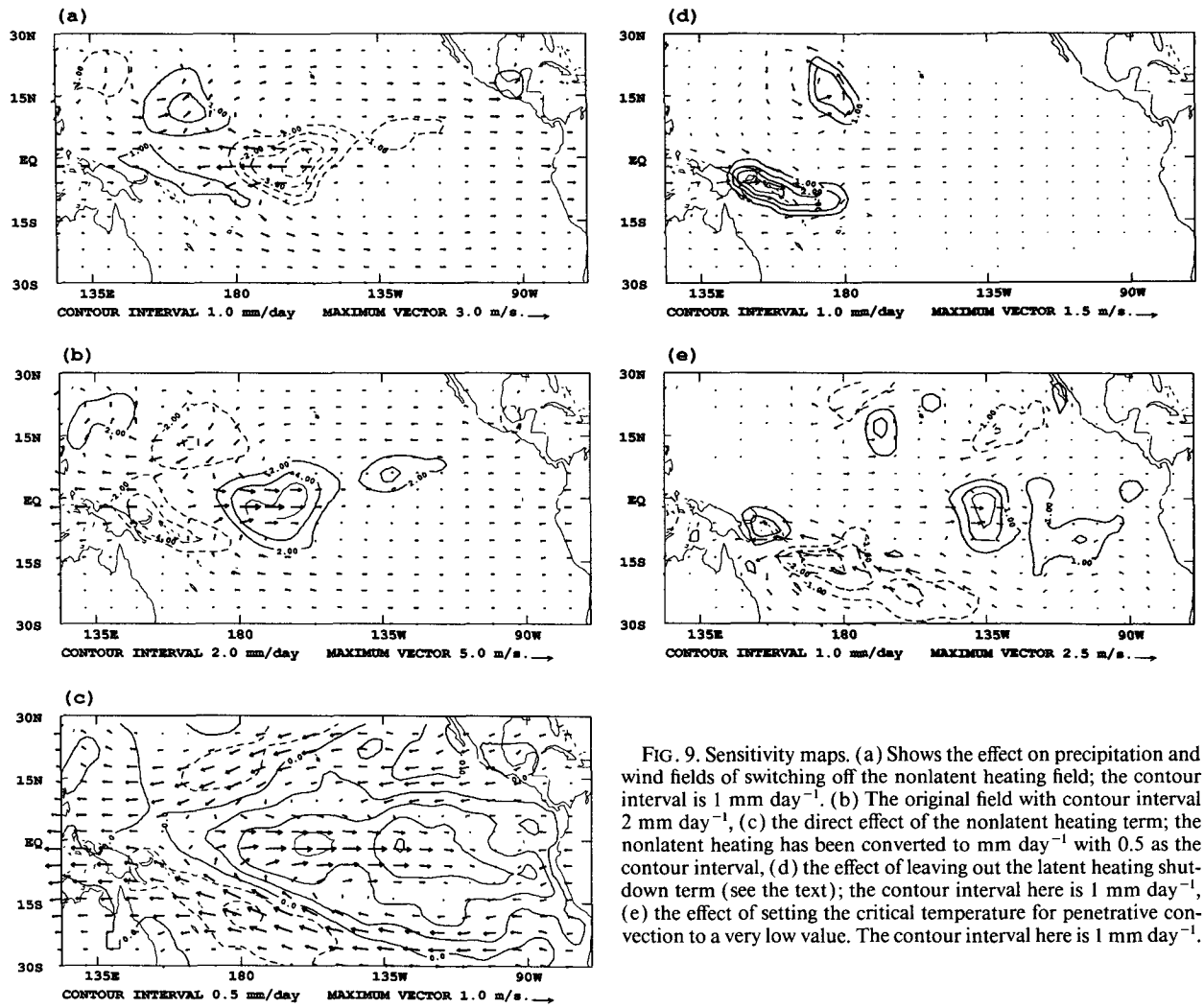

FIG. 9. Sensitivity maps. (a) Shows the effect on precipitation and wind fields of switching off the nonlatent heating field; the contour interval is 1 mm day^{-1}. (b) The original field with contour interval 2 mm day^{-1}, (c) the direct effect of the nonlatent heating term; the nonlatent heating has been converted to mm day^{-1} with 0.5 as the contour interval, (d) the effect of leaving out the latent heating shutdown term (see the text); the contour interval here is 1 mm day^{-1}, (e) the effect of setting the critical temperature for penetrative convection to a very low value. The contour interval here is 1 mm day^{-1}.

the western Pacific are primarily off-equatorial and hence are less efficient in forcing Kelvin modes in the model. It is these modes that would presumably be responsible for causing any response in the equatorial central Pacific.

The third experiment conducted involved the critical SST for penetrative convection. This was reduced to a value such that the entire tropical domain was able to support penetrative convection. The difference that this made to the precipitation and wind field can be seen in Fig. 9e. As shown, there is a substantial effect in the region of the SPCZ where the previous area of suppression (cf. Fig. 9b) has been shifted towards the southeast and overall it appears that the suppression effect has been strengthened. Associated with this effect there has been a strengthening in the southeast to easterly flow in the region of the SPCZ. This strengthening is more in accord with observations (cf. Fig. 3) and suggests that if the critical SST were to drop as latitude increased, better agreement with observations might result. A similar improvement in higher latitudes was noted when the same experiment was conducted on the 1983 case.

In the equatorial eastern Pacific there has been an increase in precipitation particularly south of the equator. At the same time, quite weak westerly anomalies have extended to the east. Both of these changes run counter to the observational evidence (although clearly the changes in wind are very marginal). A similar deterioration was noted in the 1983 case (not shown). A similar experiment in which the SST cutoff was increased to 28.7°C was also carried out for the 1987 case. In this case a slight improvement in the precipitation field was observed in the equatorial region around 135°W. This suggests that the value chosen for the SST cutoff (at least in 1987) may be slightly too low in the equatorial region.

Despite the small deterioration in agreement due to the removal of the SST cutoff, the positive anomalous precipitation response is still strongly concentrated in

the region 180°–145°W and in the region of the ITCZ (notice there is little change in these regions when the critical SST is eliminated). This is somewhat surprising given that the greatest SST anomalies are centered on the equator around 130°W (cf. Fig. 9c). In the final two experiments this feature of the response without SST cutoff was explored.

A possibility for the western and northern concentration of the response is the fact that the moisture convergence feedback parameter is higher toward the west since the total SST in this region is higher and so therefore is $\bar{q}_4 + q'_4$. To test this, the dependence of this parameter on total SST was eliminated with $\bar{q}_4 + q'_4$ set equal to 16 g kg^{-1} (an equivalent SST of $\approx$26°C) everywhere. The resulting fields and their differences from the varying parameter case can be seen in Fig. 10. As can be seen from the difference fields, there is a significant reduction in the western response with the dateline wind anomalies reduced by perhaps 25% and the precipitation just to the west of this reduced by up to 40%. An inspection of the total precipitation field shows that there are still significant departures in the response from the SST anomaly field; the positive precipitation anomalies are still concentrated on the west and north side of the SST anomalies.

A second possibility for the deviation of the precipitation response from the SST anomaly field is that the other terms in the perturbation moisture Eq. (2.4) may be biasing the response. To test this, the fixed feedback parameter experiment above was modified by eliminating all terms in the perturbation moisture Eq. (2.4) except the moisture convergence due to anomalous flow [term (3)]. The resulting fields and their differences from the original no SST cutoff experiment (Fig. 9e) are displayed in Fig. 11. Comparing the precipitation field with the SST anomalies in Fig. 9c now reveals a high degree of agreement. The difference fields indicate that the western and northern responses are significantly more suppressed than in the previous experiment. This result is perhaps not surprising given the small but significant sensitivity of the model to the various terms in the moisture equation discussed at the beginning of this section; the advection term (5) is particularly active in the western part of the model response. It is perhaps worth pointing out that if the response were to move out over the peak of the SST anomalies and thereby reduce the westerly anomalies around the dateline there would be less cancellation by the other advection term (6) since it depends on the wind anomaly while (5) does not. Physically the reason for the activity of the advection terms on the western side of the SST anomaly is because advection is a significant moisture sink in the central Pacific trades. When an SST anomaly is introduced, which peaks in the eastern Pacific, the gradient of moisture

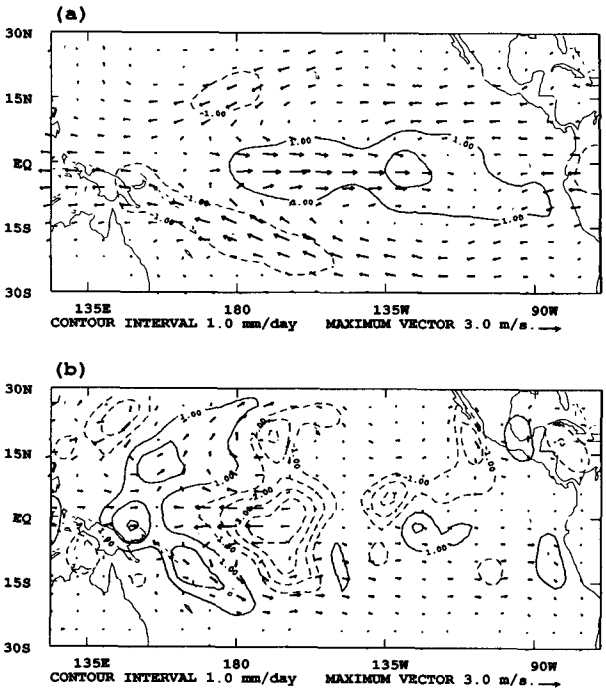

FIG. 11. The same as Fig. 10 except that now all terms but the anomalous divergence term in the perturbation moisture equation have been suppressed (see text). (a) The actual field, (b) the difference from Fig. 9e. The contour interval is 1 mm day^{-1}.

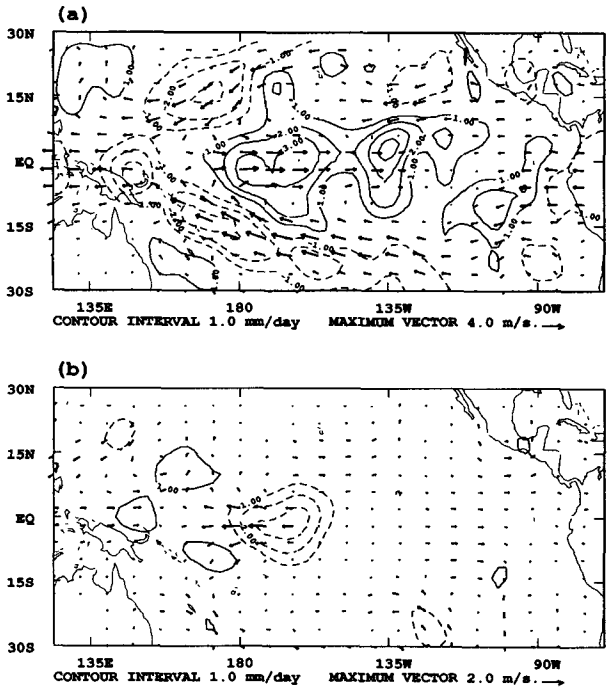

FIG. 10. This shows the effect of a very low critical temperature for penetrative convection combined with a constant coefficient for the anomalous divergence term in the perturbation moisture equation (see the text). (a) The actual field while (b) represents the difference between this and Fig. 9e. The contour interval is 1 mm day^{-1}.

(which is responsible for the advection term) is reduced on the western side of the anomaly and thus the moisture sink is reduced in this region, also. Hence, the effect on anomalous precipitation.

5. The direct thermal forcing

Perhaps the crudest physical parameterization adopted in the current model is that of the direct thermal forcing [the term $-\epsilon(RT'_4/2)$ in Eq. (2.1)]. Although, as was pointed out in section 2, this parameterization has been widely used in the literature, little discussion of its physical basis has been given. The physical processes represented by it are undoubtedly complex involving such things as radiation, convective lapse adjustment, and sensible heat transfers. This section considers only why the current crude parameterization produces effects that are similar to ones stemming from a somewhat more realistic treatment.

A more complex parameterization is based on the following two premises:

1) The upward sensible heat flux is reduced to a small fraction of its surface level value at the limit of shallow convective activity (approximately 700 mb). Within this layer there is reasonably rapid mixing.

2) The radiative equilibrium relaxation time scale is around ten times the Newtonian cooling time scale assumed in section 2. This is based on the calculations of Schneider and Lindzen (1977).

A simple calculation based on these assumptions leads one to the conclusion that the direct thermal heating is at a lower level than that implied by the current parameterization. In order to model this, a further low-level layer is inserted into the dynamical model described in section 3. The low-level geopotential and velocities are now calculated at 675 and 925 mb and the vertical velocity and temperature at 850 mb. Consistent with the above two assumptions, it is assumed that the temperature equations are as follows:

$$\omega_4 S_4 = \rho_s c_H |W|(T'_6 - \theta_4)/z_m \bar{\rho}_m \qquad (5.1)$$

$$\epsilon\theta_2 + \omega_2 S_2 = 0.1\epsilon T'_6 \qquad (5.2)$$

where the subscripts 2, 4, and 6 refer to 500, 850, and 1000 mb, respectively; c_H, $|W|$, $\bar{\rho}_m$ and z_m are the sensible heat exchange coefficient, scalar wind, mean mixed layer density, and mixed layer depth, respectively. The quantity S represents the mean potential temperature gradient at the relevant level. The following results are sensitive to this parameter in the lower layer. A value $S_4 = 2.5 \times 10^{-4}$ °K Pa^{-1} was used which is not unreasonable for the trade wind regime (see Riehl 1979, p. 231). The quantity S_2 was set at the value used previously in section 2 (6.25×10^{-4} °K Pa^{-1}). Note that we are assuming rapid Newtonian cooling to zero in Eq. (5.2). The results of this section are insensitive to this cooling parameter. The following numerical values were assumed for the other parameters in the above model: $c_H = 1.2 \times 10^{-3}$; $|W| = 5.5$ m s^{-1}; $\bar{\rho}_m = 0.85\rho_s$; and $z_m = 3 \times 10^3$ m.

With the above choice of parameters and upon assuming that the momentum equations at each level are the same as those used in (2.1), a vertical mode decomposition was carried out (see Kleeman 1989) and it was found that the two modes considered in section 2 reappeared with approximately the same structure; the physically important mode, which is retained in section 2, had a slightly reduced shallow-water speed and slightly different vertical structure. A third mode also appeared and this had a shallow-water speed of around 17.9 m s^{-1} with a vertical structure (0.023, −0.421, 0.907) where the notation means the projection of the mode onto velocities (or geopotentials) at the levels 250, 625, and 925 mb, respectively. As can be seen, this mode represents a shallow circulation.

The different vertical structure for this new mode has implications for the moisture convergence it induces. Assuming that the vertical profile discussed above applies to the entire layer in which the level is located (as assumed by the mass continuity equation) and that the humidity profile given in the Appendix applies, the value of I_2 in Eq. (2.4) is reduced from 223.25 to 58.3 mb g^{-1}.

When the vertical modes previously discussed were forced with the source functions on the right-hand side of (5.1) and (5.2), it was found that the usual deep mode is forced at around one-seventh the rate assumed in section 2. On the other hand, the third mode is quite strongly stimulated and the circulation below 500 mb is dominated by its effects.

In order to examine the implications of this circulation, the forcing implied by the SST anomalies of June–August 1987 was applied to the third mode and the resulting 925-mb circulation together with the penetrative precipitation changes resulting *directly* (i.e., before latent heat feedback) from this circulation were calculated and can be seen in Fig. 12a. The analogous quantities for the original parameterization (1000-mb circulation) are displayed in Fig. 12b. As can be seen, in the region of greatest positive precipitation anomaly (on the equator just west of the dateline) the two parameterizations produce broadly similar anomalies. Some differences can be seen in the off-equatorial regions with the more sophisticated parameterization tending to be less active particularly in the ITCZ and SPCZ. The difference in negative anomalies in the SPCZ is not greatly significant because in the model developed in section 2 the negative anomalies that result after feedback are primarily caused due to the suppression of convection caused by the SST dropping below the critical value for convection (cf. Fig. 9d).

As far as the circulation implications are concerned, it can be seen that the surface winds are somewhat strengthened. This effect amounts to around 1 m s^{-1} in the peak of westerly anomalies. In addition, the circulation is less zonal than previously and there is also

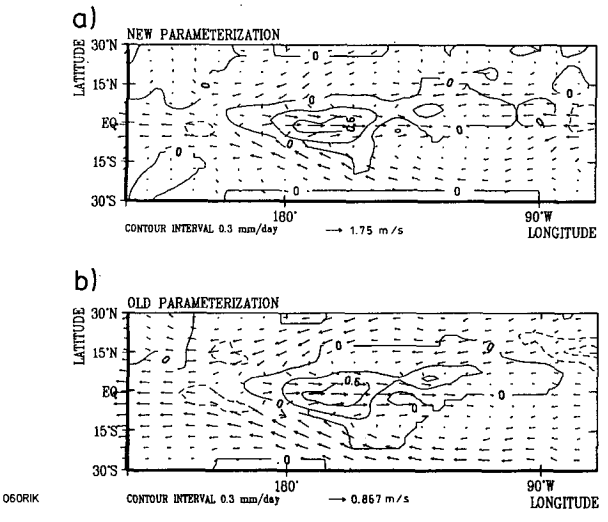

FIG. 12. The low-level circulation and direct penetrative precipitation implications of the direct thermal parameterization (5.1) and (5.2) (Fig. 12a) and the original parameterization of (2.1) (Fig. 12b). The circulation in 12(a) is at 925 mb while that in 12(b) is at 1000 mb.

some strengthening in the circulation in the ITCZ and SPCZ.

As mentioned previously, the aforementioned results show some sensitivity to the value chosen for S_4. Varying this parameter from 2.0×10^{-4} to 3.0×10^{-4} resulted in a change in precipitation of around 60% in the dateline area while the surface winds changed by around 25%. This sensitivity suggests that to further improve the parameterization of (5.1) and (5.2), better resolution is required in the mixed layer since the mean vertical potential temperature gradient varies quite significantly there. In addition, improvements could be made in the momentum equations with the incorporation of wind stress and mixing effects. Such a model is currently under development.

Despite these limitations, the aforementioned model results encourage one in the belief that the crude physical parameterization of thermal effects adopted in Eq. (2.1) is roughly correct in its implications for penetrative precipitation.

It is of some interest to compare the model of (5.1) and (5.2) with that of Lindzen and Nigam (1987). The model developed in this section differs in two respects: First, vertical temperature advection is assumed to be an important thermodynamical process in the low layers of the atmosphere while it is not in the model of Lindzen and Nigam. Second, the current model simulates the entire atmosphere while the Lindzen and Nigam model is of the low-level trade wind layer.

6. Summary and discussion

A simple model has been developed that gives a reasonable account of the tropical wind and precipitation anomalies which result from tropical sea surface temperature anomalies. The model has been tested using actual SST anomalies from various phases of ENSO and appears to be quite robust in its agreement with observations.

The model consists of a linear one vertical mode steady-state dynamical component which is forced by two types of heating anomalies: a nonlatent heating part which is a modeling of the direct thermal affect of the SST anomaly on the atmosphere, and a latent heating component which is assumed to result from changes in deep convective precipitation. In the model, this latter kind of precipitation is only allowed when the total SST is above a critical value (28°C). Outside such high SST areas precipitation is assumed to be dynamically inactive.

Precipitation changes can result from changes in the circulation and specific humidity fields, in which case they are calculated from the vertically integrated steady-state moisture equation. In addition they can result from the SST dropping below its critical value. The basic state precipitation is then used to calculate the resulting anomaly.

In the sensitivity experiments conducted on the model, it was found that while the nonlatent heating contributes only about 20% of the total response, its removal results in the total response being reduced by about 70%. Given its importance to the total response, a high priority for future improvement of the model is a more sophisticated parameterization than (2.1) including some form of simple boundary layer. Of some interest is the fact that unlike the model of Zebiak (1986), evaporative changes appear to be of minor importance in determining the total response of this model.

In comparing the model precipitation response with its forcing SST anomalies for the southern winter of 1987, it was observed that there were significant differences in the location of the two fields with the model deep convection being located mainly to the west and to a lesser extent the north of major SST anomalies. There were, in fact, large SST anomalies around 130°W on the equator which caused no local response in the deep convection. This "relocation" of the response was in good agreement with observations. Three factors in the model were found responsible for this characteristic: The 28°C cutoff in deep convection was the immediate cause with a large amount of the 130°W centered anomaly, not being sufficient to allow a response. However, even without this cutoff in the model, the response was still concentrated to the west and north (although somewhat less so). This could be traced, first, to the variability in the coefficient for anomalous divergence in the perturbation moisture equation (the so-called moisture convergence feedback parameter of Zebiak 1986), which was larger to the west and north; and second, to the other terms in this moisture equation which tended to be more active in regions to the north

and west (particularly the advection of moisture on the anomalous specific humidity gradient). The mechanism involving the variability of the feedback coefficient is very similar to that proposed by Neelin and Held (1987) for positioning convection over high SST regions; the feedback parameter [cf. Eq. (A.3)] is simply the quotient of the low-level moist static energy and a quantity proportional to the mean difference in dry static energy between the lower and upper levels of the atmosphere [see Kleeman (1989) for the relationship between c^2 and this latter quantity].

Thus, in comparison with the previous perturbation models of Zebiak (1986) and Neelin (1990) the following differences may be noted: the Zebiak model contains none of the previous three mechanisms for relocating the atmospheric response to regions of high mean SST. It relies instead on a varying anomalous evaporation, which is higher for a given SST anomaly in high mean SST regions *and* in restricting feedback to regions where the anomalous convergence exceeds any mean divergence. The Neelin model contains a mechanism very similar to the varying feedback described above but does not contain the other two mechanisms.

The previous discussion suggests that the current model may be of assistance in improving the response of coupled models such as those of Cane and Zebiak (1987) and Schopf and Saurez (1988). Both models have the atmosphere, in general, responding too far to the east. Given the large changes in the thermodynamical properties of the equatorial Pacific Ocean as one moves from the central to the east Pacific (the thermocline shoals considerably) the correct positioning of the atmospheric response may be of some importance in coupled experiments.

An intercomparison between the current models' behavior and that of Zebiak was carried out for June–August 1987 and September–November 1975. The output for Zebiaks' model forced with the appropriate CAC anomalies may be found in Fig. 13. The absolute value of the precipitation anomalies depicted should be ignored as the Zebiak model has a different vertical structure to the current model. Concentrating first on the 1987 case, two major differences are apparent between the two models (cf. Fig. 3a): in the Zebiak model, the positive precipitation anomalies are far more dominant than the negative anomalies. Second, the Zebiak model produces extensive easterly wind anomalies in the eastern Pacific which are of the same magnitude as the westerly anomalies near the dateline. This is not the case in the current model and appears to have little support in the observations.

In the 1975 case there are also significant differences between the two models (cf. Fig. 4a): relative to the positive precipitation anomalies of 1987, the negative anomalies of 1975 are far weaker, unlike the current model where the magnitude of the two anomalies are comparable. Consistent with this, the Zebiak model

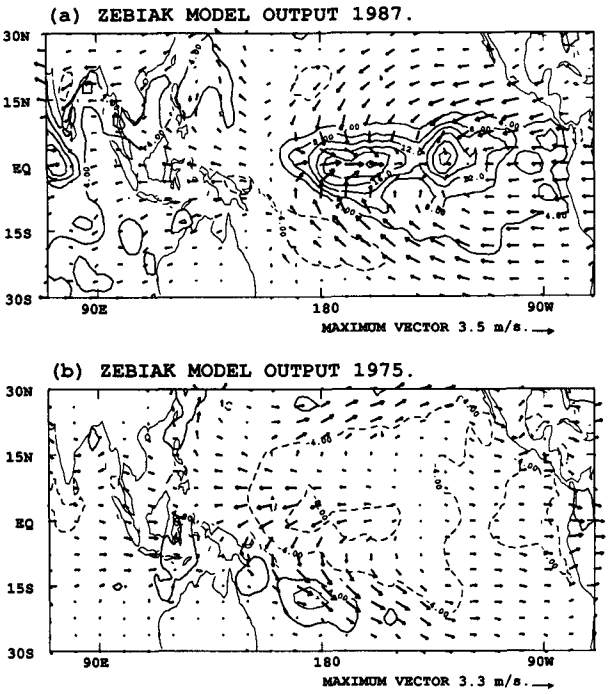

FIG. 13. The Zebiak model precipitation and surface wind anomalies for June–August 1987 (Fig. 13a) and September–November 1975 (Fig. 13b). The absolute value of the precipitation should be ignored as it refers to the current models' vertical structure.

produces easterly wind anomalies at least a factor of two weaker in the western Pacific than the current model and observations. The northwesterly anomalies in the SPCZ appear stronger than these easterlies in the Zebiak model. This is not the case in the current model or the observations.

A number of improvements to the model described here are under consideration. First, as was detailed in section 5, a better modeling of the lower layers of the atmosphere would allow a more realistic treatment of the direct thermal effects of SST anomalies. It would also allow the inclusion of Ekman layer effects which may be of importance to the moisture equation. Second, the fixed SST cutoff adopted in the model could be made meridionally dependent. Physical arguments given in section 2 and observational evidence given in section 4 both suggest that this would lead to better model performance. Finally, a dynamical linearization about the actual climatological state rather than an at rest state would appear to be an obvious step. There may be significant effects in this regard in the Indian monsoon regime where the Somali jet and associated features could be expected to have some impact. In this regard it is perhaps worth noting that the present model performed least well in that region. In connection with this, Webster (1981) has demonstrated that in certain circumstances the horizontal advection terms in the thermodynamical equation become significant.

APPENDIX

Vertical Structure Functions

The vertical dependencies of the variables used in section 2 are as follows:

$$q(p) = \begin{cases} \rho(p)\exp[(p-1000)/p_q], & p > 200 \text{ mb} \\ 0, \quad \text{otherwise} \end{cases}$$

$$u(p) = \begin{cases} \sqrt{2}\cos[\pi(1000-p)/1000], & p < 910 \text{ mb} \\ \sqrt{2}\cos(0.09\pi)\ln[(1001-p)/p_s] \\ \quad \times (\ln[(1001-910)/p_s])^{-1}, \\ \quad \text{otherwise } p_s = 2.35 \times 10^{-4} \text{ mb} \end{cases}$$

$$P(p) = \begin{cases} \sin[\pi(1000-p)/800], & \text{if } p > 200 \text{ mb} \\ 0, \quad \text{otherwise} \end{cases}$$

$$\rho(p) = [100p/RT(p)][RT(1000)/100\,000]$$

$$T(p) = \left(\frac{p}{1000}\right)^{2/7}[300 + 6.25 \times 10^{-2}(1000-p)]. \tag{A.1}$$

Note that pressure is measured in millibars and that to calculate $T(p)$ a constant $\overline{\partial\theta/\partial p}$ is assumed. [The assumption made in the dynamical part of the model (see Kleeman 1989)]. The parameter p_q is a scale height for the moisture field and a value of 400 mb gives reasonable agreement with observations of the lower tropical troposphere (see Newell et al. 1972). The particular form for $\mathbf{u}(p)$ below 910 mb was chosen to roughly simulate boundary layer behavior. The 1000 mb value is 70% of the 850 mb value.

With the above functional forms the vertical structure integrals have the values

$$gI_2 = 223.25 \text{ mb}$$

$$gI_1 = 669.35 \text{ mb m}^{-3} \text{ kg}. \tag{A.2}$$

It is worth noting that the moisture convergence feedback parameter [discussed by Gill and Davey (1987) and by Zebiak (1986)] is given by

$$\beta = RL_v I_2(\bar{q}_4 + q'_4)/2c_p\rho_2 I_1 c^2. \tag{A.3}$$

For the choice of parameters made here, this quantity is 0.956 when the surface specific humidity is 20 g kg^{-1}, a value achieved when the SST is approximately 30.2°C. Experimentation with this parameter showed that divergence in the iteration process occurred when its value was increased to a value slightly above one. For the values of SST encountered in the datasets used here such values were never encountered and no evidence of iterative divergence was ever observed.

REFERENCES

Anderson, D. L. T., and J. P. McCreary, 1985: Slowly propagating disturbances in a coupled ocean–atmosphere model. *J. Atmos. Sci.*, **42**, 615–629.

Arkin, P. A., and B. N. Meisner, 1987: The relationship between large-scale convective rainfall and cold cloud over the western hemisphere during 1982–84. *Mon. Wea. Rev.*, **115**, 51–74.

Battisti, D. S., 1988: Dynamics and thermodynamics of a warming event in a coupled tropical atmosphere ocean model. *J. Atmos. Sci.*, **45**, 2889–2919.

Budin, G. R., and M. K. Davey, 1989: A simple tropical coupled ocean–atmosphere model. British Meteorology Office Dynamical Climatology Tech. Note No. 75, (Available from London Road, Bracknell, Berkshire RG12 2SZ).

Cane, M. A., and S. E. Zebiak, 1987: A model El Niño Southern Oscillation. *Mon. Wea. Rev.*, **115**, 2262–2278.

Davey, M. K., and A. E. Gill, 1987: Experiments on tropical circulation with a moist model. *Quart. J. Roy. Meteor. Soc.*, **113**, 1237–1270.

Gill, A. E., 1980: Some simple solutions for heat-induced tropical circulation. *Quart. J. Roy. Meteor. Soc.*, **106**, 447–462.

——, 1985: Elements of coupled ocean–atmosphere models for the tropics. *Coupled Ocean–Atmosphere Models*, Elsevier, 303–327.

Graham, N. E., and T. P. Barnett, 1987: Sea surface temperature, surface wind divergence, and convection over tropical oceans. *Science*, **238**, 657–659.

Hirst, A. C., 1986: Unstable and damped equatorial modes in simple coupled models. *J. Atmos. Sci.*, **43**, 606–630.

Kleeman, R., 1989: A modeling study of the effect of the Andean mountains on the summertime circulation of tropical South America. *J. Atmos. Sci.*, **46**, 3344–3362.

Lee, D. M., and J. V. Maher, 1977: Upper-air statistics Australia. *Meteorological Summary*, Bureau of Meteorology, Melbourne 3000, Australia.

Lindzen, R. S., and S. Nigan, 1987: On the role of sea surface temperature gradients in forcing low-level winds and convergence in the tropics. *J. Atmos Sci.*, **44**, 2418–2436.

Neelin, D. J., 1988: A simple model for surface stress and low-level flow in the tropical atmosphere driven by prescribed heating. *Quart. J. Roy. Meteor. Soc.*, **114**, 747–770.

——, 1990: A hybrid coupled general circulation model for El Niño studies. *J. Atmos. Sci.*, **47**, 674–693.

——, and I. M. Held, 1987: Modeling tropical convergence based on the moist static energy budget. *Mon. Wea. Rev.*, **115**, 3–12.

Newell, R. E., J. W. Kidson, D. G. Vincent and G. J. Boer, 1972: *The General Circulation of the Tropical Atmosphere. Vol. 1.* The MIT Press.

Oort, A. H., 1983: Global atmospheric circulation statistics, 1958–1973. NOAA Professional Paper 14, U.S. Department of Commerce, Chap. 5. Washington,

Riehl, H., 1979: *Climate and Weather in the Tropics.* Academic Press,

Schneider, E. K., and R. S. Lindzen, 1977: Axially symmetric steady-state models of the basic state for instability and climate studies. Part I: Linearized calculations. *J. Atmos Sci.*, **34**, 263–279.

Schopf, P. S., and M. J. Suarez, 1988: Vacillations in a coupled ocean–atmosphere model. *J. Atmos Sci.*, **45**, 549–566.

Weare, B. C., 1986: A simple model of the tropical atmosphere with circulation dependent heating and specific humidity. *J. Atmos. Sci.*, **43**, 2001–2016.

Webster, P. J., 1981: Mechanisms determining the atmospheric response to sea surface temperature anomalies. *J. Atmos. Sci.*, **38**, 554–571.

Zebiak, S. E., 1986: Atmospheric convergence feedback in a simple model for El Niño. *Mon. Wea. Rev.*, **114**, 1263–1271.